Functional Sensitivity and Mutational Robustness of Proteins

Qian-Yuan Tang,* Testsuhiro S. Hatakeyama, and Kunihiko Kaneko†
Center for Complex Systems Biology, Universal Biology Institute, University of Tokyo, Tokyo, Japan.
(Dated: June 19, 2020)

Sensitivity and robustness appear to be contrasting concepts. However, natural proteins are robust enough to tolerate random mutations, meanwhile be susceptible enough to sense environmental signals, exhibiting both high functional sensitivity (i.e., plasticity) and mutational robustness. Uncovering how these two aspects are compatible is a fundamental question in the protein dynamics and genotype-phenotype relation. In this work, a general framework is established to analyze the dynamics of protein systems under both external and internal perturbations. We introduce fluctuation entropy for the functional sensitivity and the spectrum entropy for the mutational robustness. The compatibility of sensitivity and robustness is analyzed by the optimization of two entropies, which leads to the power-law vibration spectrum of proteins. These power-law behaviors are confirmed extensively by protein data, as a hallmark of criticality. Moreover, the dependence of functional sensitivity and mutational robustness on the protein size suggests a general evolutionary constraint for proteins with different chain lengths. This framework can also establish a general link of the criticality with robustness-plasticity compatibility, both of which are ubiquitous features in biological systems.

I. INTRODUCTION

Proteins are highly dynamic molecules in living cells [1–4]. As a living system, a protein molecule is subjected to external and internal perturbations. For proteins in the solutions, small external perturbations from the milieu can be felt consistently by every other residue within the entire protein. Even weak and transient perturbations can trigger large conformational changes [5–8]. In this way, proteins can sense external signals ranging from metal ions to other biomolecules, which are functionally beneficial.

Meanwhile, internal perturbations also affect proteins. Numerous mutations occur intermittently in gene sequences encoding amino acid residues of proteins. In the "sequence-structure-dynamics-function" paradigm [9, 10], mutations may change the native protein structure; consequently, the equilibrium dynamics and corresponding biological functions will be affected. However, accumulating evidence has shown that protein molecules can tolerate numerous types of amino acid substitutions and maintain their thermodynamic stability and folding pathways [11–15]. Besides, the principal components of protein equilibrium dynamics are highly robust to minor structural differences or detailed atomic-level interactions [9, 16–19]. These results demonstrate that the dynamics of proteins are highly robust to mutations.

Indeed, both high sensitivity to external perturbations and high robustness to internal perturbations are essential for protein systems. Proteins without a high functional sensitivity cannot respond transiently or undergo large-scale conformational changes. Meanwhile, without high mutational robustness, the functional proteins with high fitness cannot be stably replicated or inherited. However, the former and latter concern changeability and non-changeability, respectively, and may direct us to different ends [20–23]. Thus, uncovering the link between the two aspects is essential for understanding the genotype-phenotype relation of the proteins. Native-state dynamics and corresponding responses to noises and mutations may provide the key to it.

In this paper, with a simplified protein model, we establish a general framework for analyzing protein dynamics, which is subjected to external and internal perturbations. We introduce the fluctuation entropy and spectrum entropy to describe the functional sensitivity and mutational robustness, respectively. Then, from the perspective of the vibration spectrum, the interplay between functional sensitivity and mutational robustness of proteins is analyzed. In systems with low degrees of freedom, the two entropies act as consistent descriptors. However, in systems with high degrees of freedom, the interplay between functional sensitivity and mutational robustness will lead to a power-law eigenvalue distribution in the relaxation dynamics. Such a power-law distribution is supported by the vibration spectra of natural proteins. The corresponding power-law coefficient is closely associated with the packing density of protein molecules. The size dependence of functional sensitivity and mutational robustness suggests a general evolutionary constraint for proteins with different sizes.

II. FUNCTIONAL SENSITIVITY AND MUTATIONAL ROBUSTNESS

A. Model

Globular proteins fold into their native structure to perform their biological functions. For proteins fluctuating around their equilibrium configuration, the relax-

* tang@complex.c.u-tokyo.ac.jp
† kaneko@complex.c.u-tokyo.ac.jp

ations and fluctuations can be captured by linear models. By approximating the energy landscape around the native state in the quadratic form, potential energy

$$V(\Delta\vec{r}) = \frac{\gamma}{2} \cdot \Delta\vec{r}^T \cdot \mathcal{H} \cdot \Delta\vec{r}, \tag{1}$$

in which $\Delta\vec{r} = [\Delta r_1, \Delta r_2, \cdots \Delta r_N]^T$ is a vector describing the displacement of all N residues deviating from the native structure, and $\mathcal{H}$ is the second-order derivative of potential energy, known as the Hessian matrix. In this way, a protein molecule can be modeled into an elastic network, where amino acid residues (represented by nodes positioned at their C_α atom) are connected via elastic springs [24]. As a simple yet powerful model, elastic networks are applied widely for elucidating the functional dynamics [25, 26] and evolutionary constraints [27–30] of proteins.

Additionally, after assuming that all residue fluctuations are Gaussian variables distributed around their equilibrium coordinates, Gaussian Network Model (GNM) is introduced to describe the fluctuations around native protein structures [31, 32]. In the GNM, the Hessian matrix $\mathcal{H}$ can be reduced as the graph Laplacian, describing the topology of the elastic network. The structural fluctuations around the native state can then be described by a multivariate Gaussian distribution [17], given by

$$\phi(\Delta\vec{r}) = \frac{1}{(2\pi)^{3N/2}(\det\mathcal{H})^{-3/2}} e^{-\frac{3\gamma}{2k_T}\Delta\vec{r}^T\cdot\mathcal{H}\cdot\Delta\vec{r}}, \tag{2}$$

where γ, k_B, and T denote the spring constant, Boltzmann constant, and temperature, respectively.

Based on the GNM, normal mode analysis (NMA) can provide essential information about thermal fluctuations, large-scale conformational dynamics, and linear responses of native proteins [33–36]. Upon performing the eigenvalue decomposition of the Hessian matrix $\mathcal{H}$, the normal modes described by eigenvectors $(\vec{v}_0, \vec{v}_1, \vec{v}_2, \cdots, \vec{v}_{N-1})$ and corresponding eigenvalues $(0 = \lambda_0 < \lambda_1 \leq \lambda_2 \leq \cdots \lambda_{N-1})$ can be obtained. Notably, the matrix $\mathcal{H}$ is positive semi-definite; there is always $\lambda_0 = 0$, showing the translational invariance of the system. The native dynamics of proteins can then be described as a linear combination of independent normal modes.

B. Functional sensitivity

Here, we introduce "functional sensitivity" to quantify that how much will an external perturbation leads to the deformations of a protein molecule. For native proteins, high functional sensitivity usually correlates with low structural robustness, and it is closely associated with the geometry at the native basin of the energy landscape. Molecular simulations have proved that energy landscapes of proteins are highly anisotropic along different directions [37–39]. In NMA, the eigenvalue magnitudes provide information about the local curvature of the energy landscape along the direction of the corresponding eigenvectors [40]. An illustrative energy landscape is shown in Fig. 1A. Here, $\lambda_j < \lambda_k$ indicates that the motion along $\vec{v_j}$ is more easily accessible, and lesser energy is needed to excite such deformations, as compared to that for the motion along the direction of $\vec{v_k}$. To quantify the functional sensitivity of a protein molecule, one shall measure the total "volume" of the accessible configuration space at the given perturbation level (temperature). To calculate that, we introduce the fluctuation entropy S_F of the protein molecule as the Shannon entropy (or differential entropy) [41–43] of the fluctuation distribution $\phi(\Delta\vec{r})$.

$$\begin{aligned} S_F(\Delta\vec{r}) &= -\int \phi(\Delta\vec{r}) \log \phi(\Delta\vec{r}) d\Delta\vec{r} \\ &= 3Ns_0 - \frac{1}{2}\log\prod_{i=1}^{N-1}\lambda_i = 3Ns_0 - \frac{1}{2}\sum_{i=1}^{N-1}\log\lambda_i, \end{aligned} \tag{3}$$

in which $s_0 = \frac{1}{2} \cdot \log\left(\frac{2\pi k_B T}{\gamma}\right)$. According to such an expression, the fluctuation entropy of protein molecules can be decomposed into two parts: a constant term and another term equal to the logarithm of the product $\prod_{i=1}^{N-1}\lambda_i^{-1}$. This product is also known as the pseudo-determinant of the matrix $\mathcal{H}$ [44]. For the j-th normal mode, the λ_j^{-1} describes variance along the direction of the eigenvector $\vec{v}_j$. As illustrated in Fig. 1A, the pseudo-determinant can be understood as the volume of the configuration space; the fluctuation entropy is the logarithm of such a volume.

The physical meaning of the fluctuation entropy S_F is clear: when there are more eigenvalues with small magnitude, the corresponding slow-mode motions will be easier to activate. The fluctuation entropy of such a molecule is high, indicating that a small perturbation can lead to large fluctuations in such a system. It is worth noting that the fluctuation entropy is consistent with other measures for system sensitivity, such as the condition number. Such consistency is discussed in the Supplementary Materials (SM).

C. Mutational robustness

In living cells, mutations happen from time to time. For a protein system, the mutations can be understood as internal perturbations. Mutations in the sequence may cause changes in protein structures. However, structural differences or residue-residue interactions do not necessarily imply that the dynamics of a protein are different [16–19]. For example, the structure of the apo and holo states of an allosteric protein may differ considerably, but a conformational transition can easily connect the two states. Besides, proteins as a product of evolution can tolerate numerous kinds of amino acid substitutions and maintain their native-state structures [11–13, 15]. To

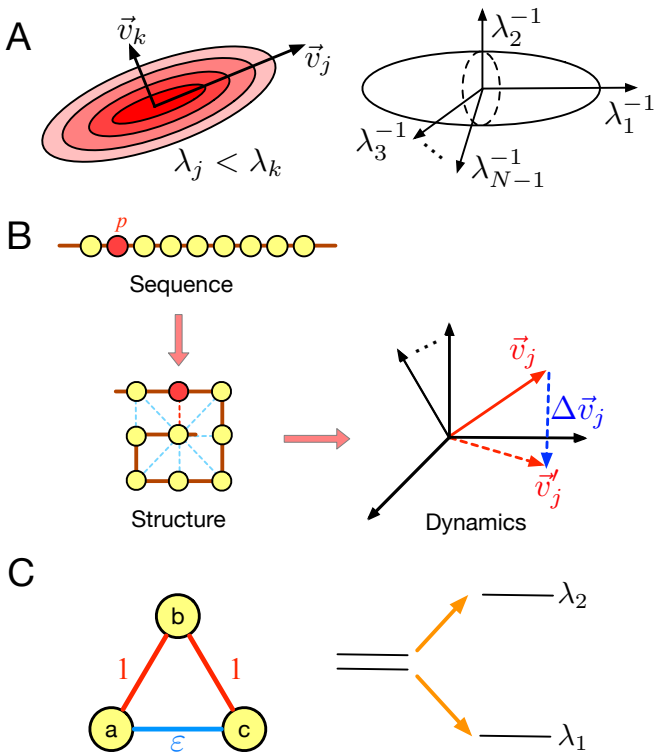

FIG. 1. Illustration of functional sensitivity and mutational robustness. (A) Left: When $\lambda_j < \lambda_k$, as compared to $\vec{v}_k$, the motions along $\vec{v}_j$ will be easier to access, and less energy is required for deformation. Right: The configuration space of the protein molecule around the native state is shown to be a high-dimension ellipsoid, in which the length of the j-th semi-axes is λ_j^{-1}. The fluctuation entropy is defined as the logarithm of this volume. (B) The original amino acid sequence folds into a specific native protein structure and exhibits specific functional dynamics. After the mutation on-site p, interactions between residue p and other neighboring residues change, and the dynamics of such a protein also change slightly. For example, the j-th eigenvector $\vec{v}_j$ will transform into $\vec{v}'_j$ after such a mutation. The difference in such an eigenvector is $\Delta\vec{v}_j$. (C) An illustrative model of the three-bead chain is shown. Here, maximizing the eigengap can contribute to both functional sensitivity and mutational robustness.

quantify the consequential effects (changes in the phenotype) of mutations, in this work, we mainly focus on the robustness of the native dynamics of the protein [45, 46].

As discussed above, the native dynamics of a protein can be described as a linear combination of eigenvectors of the Hessian matrix $\mathcal{H}$. Hence, changes caused in protein native dynamics owing to mutations can be simplified as differences in eigenvectors of such a system. As illustrated in Fig. 1B, a mutation in residue i changes its interactions with neighboring residues. These changes will affect the elements of the Hessian matrix $\mathcal{H}$. When a mutation happens on site p, the Hessian matrix changes from $\mathcal{H}$ to $\mathcal{H}'$, where $\mathcal{H}' = \mathcal{H} + \epsilon M$. Here, the parameter ϵ denotes the perturbation magnitude, and M is a symmetric perturbation matrix that describes changes in inter-residue interactions. After the mutation, the eigenvalues of the Hessian matrix shift from $\lambda_1, \lambda_2, \cdots \lambda_{N-1}$ to $\lambda'_1, \lambda'_2, \cdots \lambda'_{N-1}$, respectively, and the corresponding eigenvectors change from $\vec{v}_1, \vec{v}_2, \cdots \vec{v}_{N-1}$ to $\vec{v}'_1, \vec{v}'_2, \cdots \vec{v}'_{N-1}$, respectively.

To characterize the robustness of equilibrium dynamics in a protein molecule, one needs to check if the mutation can easily modify the eigenvectors closely associated with the functional motion of such a protein. If a protein can maintain its function-related eigenvectors after a mutation, such a protein shows high mutational robustness in the evolutionary process.

Without the loss of generality, let us assume that the j-th eigenvector is most closely associated with the functional motion of the protein. According to the first-order perturbation theory [47], the perturbed eigenvector $\vec{v}'_j$ can be expressed as:

$$\vec{v'_j} = \vec{v}_j + \Delta\vec{v}_j = v_j + \epsilon \sum_{i \neq j} \frac{\vec{v}_i^T \cdot M\vec{v}_j}{\lambda_i - \lambda_j} \vec{v}_j. \tag{4}$$

Therefore, for eigenvector v'_j, the square deviation is expressed as:

$$|\Delta\vec{v}_j|^2 \leq \epsilon^2 \sum_{i \neq j} \frac{||M||_2}{(\lambda_i - \lambda_j)^2} |\vec{v}_j|^2 \leq \frac{\epsilon^2 N(N-2)||M||_2}{(g_j^*)^2}, \tag{5}$$

where $||M||_2$ denotes the L_2-norm of matrix M, which is bound by the number of mutated contacts, and g_j^* denotes the minimum gap between λ_j and its neighboring eigenvalues, say, $g_j^* = \min\{|\lambda_j - \lambda_{j-1}|, |\lambda_{j+1} - \lambda_j|\}$. The magnitude of $|\Delta\vec{v}_j|^2$ can quantify the robustness of vector $\vec{v}_j$ after perturbation. Larger $|\Delta\vec{v}_j|^2$ indicates more significant changes in the dynamics of the j-th eigenvector, which implies lower mutational robustness in protein dynamics (see SM). According to Eq.5, the upper bound of $|\Delta\vec{v}_j|^2$ of the j-th eigenmode is determined by $1/(g_j^*)^2$; thus, a larger eigengap g_j^* corresponds to a higher mutational robustness of the eigenvector $\vec{v}_j$.

D. A system with low degrees of freedom

In previous discussions, we demonstrated that functional sensitivity and mutational robustness are closely related to the spectral properties of the elastic network. To illustrate the possible relationships between functional sensitivity and mutational robustness, let us first focus on a simple three-bead system with two degrees of freedom. As shown in Fig. 1C, the strength of the bonded interactions is 1, and the strength of the non-bonded interaction is ε ($0 \leq \varepsilon \leq 1$). By NMA, the non-zero eigenvalues are found to be: $\lambda_1 = 1 + 2\varepsilon$ and $\lambda_2 = 3$. To maximize the functional sensitivity, the non-bonded interaction ε shall be weakened, to ensure that the fluctuation entropy $S_F \sim -\log(\lambda_1\lambda_2)$ is maximized. To maximize the mutational robustness of the first and second eigenvectors, the eigengap $|\lambda_2 - \lambda_1|$ shall be maximized.

When $\varepsilon = 0$, both functional sensitivity and mutational robustness reach maximum. This model illustrates that in systems with low degrees of freedom, maximizing the gaps between the two non-zero eigenvalues can contribute to both functional sensitivity and mutational robustness. For example, brain networks can be coarse-grained as block models, which only have low degrees of freedom. Previous studies have proved that larger gaps between eigenvalues, which correspond to the modular organization in the brain, may confer increased robustness to network perturbations and higher flexibility in learning [48].

III. THE INTERPLAY BETWEEN FUNCTIONAL SENSITIVITY AND MUTATIONAL ROBUSTNESS FOR A SYSTEM WITH MANY DEGREES OF FREEDOM

In usual cases, the functional dynamics of a protein cannot be described by a single eigenvector, but needs to be expressed as a linear combination of a set of eigenvectors. The above discussions can also be generalized for the mutational robustness of a linear subspace (details in SM). Here, as an example, let us consider the linear subspace $\mathcal{V}_j$, spanned by the first j slow-mode eigenvectors $\vec{v}_1, \vec{v}_2, \cdots, \vec{v}_j$. It can be concluded that the mutational robustness of the linear space $\mathcal{V}_j$ will be upper bounded by the eigengap $|\lambda_{j+1} - \lambda_j|$. If we consider the linear space $\mathcal{V}$ spanned by all the eigenvectors $\vec{v}_1, \vec{v}_2, \cdots \vec{v}_{N-1}$, the mutational robustness of eigenspace $\mathcal{V}$ will be upper bounded by $g^*_{\min} = \min_j\{|\lambda_{j+1} - \lambda_j|\}$. To maximize the robustness of eigenspace $\mathcal{V}$ under mutations, the minimum eigengap $g^*_{\min}$ of the entire spectrum shall be maximized. This will lead to a uniform distribution of all the eigenvalues as long as the eigenvalues are bounded between $\lambda_{\min}$ and $\lambda_{\max}$.

To quantify the uniformity of the eigenvalue distribution, we define spectrum entropy $\mathcal{S}$ as the Shannon entropy of the eigenvalue distribution:

$$\mathcal{S} = -\int g(\lambda) \log g(\lambda) d\lambda, \tag{6}$$

Where $g(\lambda) = \frac{1}{N}\sum_i \delta(\lambda - \lambda_i)$ is the probabilistic density function of eigenvalues. This definition can also be understood as the Kullback–Leibler divergence from a uniform distribution to the given eigenvalue distribution (see SM). Notably, the maximum-entropy distribution, in the absence of other constraints, corresponds to a uniform distribution. In such a situation, the minimum eigengap $g^*_{\min}$ can be maximized to ensure that proteins show the highest mutational robustness in the eigenspace $\mathcal{V}$.

For systems with high degrees of freedom, the interplay between functional sensitivity and mutational robustness is complicated. To maximize the functional sensitivity (fluctuation entropy S_F) of a system, as illustrated in Fig. 2A, one will expect an eigenspectrum with $N-2$ vibration modes, where eigenvalues are close to zero ($\lambda_1 \approx \lambda_2 \approx \cdots \approx \lambda_{N-2} \approx 0$), and the largest eigenvalue λ_{N-1} is much larger than zero. In such a situation, the fluctuation entropy reaches the maximum, which ensures that external perturbations can easily trigger the motions of the molecule along the directions of the first $N-2$ eigenvectors. However, the gaps between low-frequency modes are expected to be very small; thus, these low-frequency modes are not stable under mutations. To maximize the mutational robustness of the linear space $\mathcal{V}$ spanned by eigenvectors, as shown in Fig. 2B, a uniform distribution is expected, to ensure that the minimum eigengap $g^*_{\min}$ is maximized. Thus, for a system with many degrees of freedom, functional sensitivity and mutational robustness are two different optimization objectives that may be hard to be compatible.

A. Entropy maximization

How can the dynamics of a protein molecule ensure that both functional sensitivity and mutational robustness are maintained? To resolve this problem, we introduced the entropy maximization approach, to analyze the spacing problems of the eigenvalue distribution. Previously, the principle of maximum entropy [49] had already been applied in protein science. The applications include protein sequence evolution [50], structural constraint identification from correlated motions [51], residue interaction deduction [52], and protein folding [53]. In practice, the entropy maximization approach can handle multiple constraints, which introduce additional information into the system.

To determine the optimal eigenvalue distribution of protein systems, we consider fluctuation entropy as a constraint and maximize the spectrum entropy. From the physical perspective, it means that we fix the high functional sensitivity of a system, and then attempt to maximize the mutational robustness of the linear space spanned by all the eigenvectors. There are three constraints in this optimization process: (a) The spectrum distribution is normalized, i.e., $\int g(\lambda)d\lambda = 1$; (b) The total number of contacts in the proteins is constant, i.e., the trace of the Hessian matrix is fixed: $\int \lambda g(\lambda)d\lambda = m$; (c) The fluctuation entropy is be fixed as a constraint $\mathcal{C}$, i.e., $\int \log\lambda \cdot g(\lambda)d\lambda = \mathcal{C}$. Such a functional constraint ensures that during the evolution process, no matter how the interactions within proteins change with mutations, the fluctuation entropy will always be constant.

Take the three constraints as multipliers, we can obtain the Lagrangian expression:

$$\begin{aligned}\hat{\mathcal{S}} = &-\int g(\lambda)\log g(\lambda)d\lambda + \zeta_0\left(\int g(\lambda)d\lambda - 1\right)\\ &+\zeta_1\left(\int \lambda g(\lambda)d\lambda - m\right) + \zeta\left(\int \log\lambda\cdot g(\lambda)d\lambda - \mathcal{C}\right).\end{aligned} \tag{7}$$

To find the distribution function $g^*(\lambda)$ that maximizes entropy $\hat{\mathcal{S}}$ across all probability distributions, we require

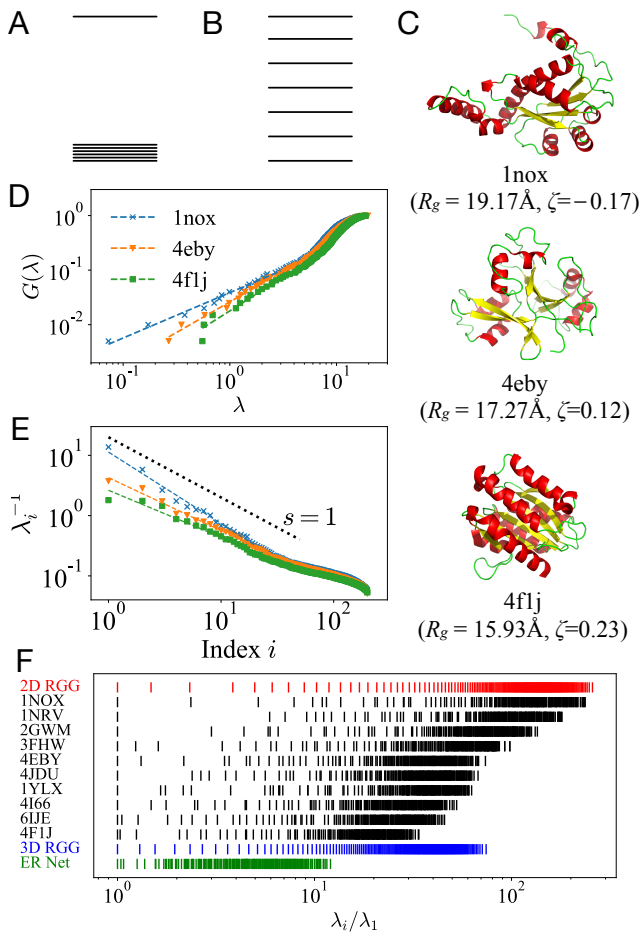

FIG. 2. (A) The eigenvalue distribution that maximizes functional sensitivity. (B) The eigenvalue distribution that maximizes the mutational robustness of the linear space spanned by all the eigenvectors. (C) The cartoon structure of the three proteins (PDB code: 1NOX, 4EBY, and 4F1J) with the same chain length ($N = 200$). (D) The integrated eigenvalue distribution function $G(\lambda)$ and (E) the magnitude of the i-th mode λ_i^{-1} vs the index (rank) i for the three proteins is shown. The dashed lines in (D) and (E) show the fitting results based on the first 20 eigenvalues of the proteins. (F) The eigenvalue spectra of proteins with chain length $N = 200$ is shown. All eigenvalues are normalized to the lowest nonzero eigenvalue λ_1, and the log-scale that clearly presents the differences between neighboring eigenvalues is selected. The spectra of proteins are compared with Erdős-Rényi networks and random geometric graphs (2D or 3D).

the following:

$$\frac{\partial \hat{S}}{\partial g(\lambda)} = -\log g(\lambda) - 1 + \zeta_0 + \zeta_1 \lambda + \zeta \log \lambda = 0, \quad (8)$$

hence $g^*(\lambda)$ can be solved as:

$$g^*(\lambda) = e^{-1+\zeta_0+\zeta_1\lambda}\lambda^{\zeta}. \quad (9)$$

Such a spectrum shows a power-law distribution with an exponential cutoff. In the slow-mode limit, when $\lambda \sim 0$, such a spectrum can be reduced into a power-law distribution: $g(\lambda) \sim \lambda^{\zeta}$, and the power-law exponent equals the Lagrangian multiplier ζ. In the fast-mode limit, the spectrum distribution will be dominated by the exponential function, which mainly results from the finite-size effect of the molecule. A similar eigenvalue distribution can be obtained by taking spectrum entropy as a constraint and maximizing the fluctuation entropy (listed in SM).

B. The eigenvalue distribution of proteins

Remarkably, the spectra of natural proteins are in good accord with the above theoretical analysis. Here, we take three proteins (illustrated in Fig. 2C) with the same chain length ($N = 200$) but different structures as examples (more examples listed in SM). Based on the vibration spectra (obtained by NMA) of proteins, the power-law coefficients can be obtained by fitting the eigenvalue distribution. Here, we consider the integrated eigenvalue distribution function $G(\lambda) = \int_0^{\lambda} g(\lambda')d\lambda'$. In the slow-mode limit, we have $g(\lambda) \sim \lambda^{\zeta}$; thus, $G(\lambda) \sim \lambda^{\zeta+1}$. As shown in Fig.2D, for the first 10 to 20 eigenvalues, $G(\lambda)$ occurs in a line in the double logarithmic scale, clearly demonstrating power-law behavior. The slope of the log-log plot of $G(\lambda)$ is used to determine the power-law coefficient $\zeta + 1$. After fitting the first 20 distribution-based eigenvalues, for the three proteins in Fig. 2C, we have $\zeta = -0.17, 0.12$, and 0.23.

Another approach for demonstrating power-law behavior is to obtain the rank-size distribution of the system. As discussed in the previous section, the magnitude of λ_i^{-1} describes fluctuations along the direction of eigenvector $\vec{v}_i$. Because $\lambda_1^{-1} \geq \lambda_2^{-1} \geq \cdots \geq \lambda_{N-1}^{-1}$, the rank-size relation of the eigenmodes is λ_i^{-1} vs the rank (eigenvalue index) i. As shown in Fig. 2E, for slow-mode eigenvalues, the rank-size distribution shows a power law, known as Zipf's law, i.e. $\lambda_i^{-1} \sim i^{-s}$, where s is the Zipf's exponent. Fitting the first 20 eigenvalues in the spectra of the three proteins, we have $s = 1.19, 0.88$, and 0.78, which are all close to 1. Such a power-law decay quantitatively demonstrates that the low-frequency normal modes contribute significantly to the equilibrium fluctuations of proteins.

It is worth noting that the eigenvalue index i is proportional to the integrated eigenvalue distribution function, because $G(\lambda_i) = \int_0^{\lambda_i} g(\lambda')d\lambda' \sim \sum_{k \leq i} \delta(\lambda_k - \lambda_i) = i$. In the slow-mode limit, $G(\lambda) \sim \lambda^{\zeta+1} \sim i \sim \lambda^{1/s}$. Thus, $\zeta = 1/s - 1$ and measured ζ and s values are consistent with the relationship: For the three proteins in Fig. 2C, when $\zeta = -0.17, 0.12$, or 0.23, $s = 1.19, 0.88$, or 0.78. For most proteins, $s \approx 1$, and $\zeta \approx 0$. Note that power-law coefficients ζ and s are closely related to the spectral dimension d_s [54] of the proteins: $d_s = 2(\zeta + 1) = 2/s$, and $d_s \approx 2 < 3$ (see SM).

In Fig. 2F, the spectra of proteins with the same chain lengths ($N = 200$) are illustrated. Although the spec-

tra of different proteins are varied, these spectra show similar behavior. At the logarithmic scale, the first 10 to 20 eigenvalues are roughly uniformly distributed, and act as a power-law distribution. The other eigenvalues are rather concentrated, demonstrating the characteristic scale of the exponential distribution. For comparison, the spectra of the Erdős-Rényi (ER) random network [55] and random geometric graphs (RGG) with a similar number of nodes and edges [56] are also shown in Fig. 2F. In comparison with ER networks, the vibration spectrum of proteins has a notable power-law distribution in the slow mode. In contrast, the spectra of these proteins are very similar to those of RGGs. For most proteins, the scales of the eigenvalues (characterized by λ_{N-1}/λ_1) [57] lie between the spectra of 2-dimensional and 3-dimensional RGG. This result is in line with those of previous studies, demonstrating that the structure of proteins can be described as the packing of amnio-acid residues in a fractal dimension between 2 and 3 [8, 54].

IV. THE COMPATIBILITY OF FUNCTIONAL SENSITIVITY AND MUTATIONAL ROBUSTNESS: CONFIRMATION BY STRUCTURAL INFORMATION

Here, based on a large data set of protein structures, we analyze the interplay between functional sensitivity and mutational robustness of proteins. For simplification, we mainly focus on the functional sensitivity and mutational robustness contributed by the first two normal modes (discussions on the other modes are listed in SM). The fluctuation entropy contributed by the first two modes can be expressed as $-\log(\lambda_1\lambda_2)$; hence, we take $1/(\lambda_1\lambda_2)$ to be a descriptor of functional sensitivity. For mutational robustness, because λ_1 and λ_2 are the smallest eigenvalues in the system, to magnify the difference between them, we introduce $|\lambda_1^{-1} - \lambda_2^{-1}|$ to describe the gap between the first and second eigenvalues.

Now, let us address the question regarding the physical meaning of the exponent ζ. We focus on a subset of proteins with similar chain lengths ($180 \leq N < 220$). Although these proteins have similar sizes, their shapes and structures are different. For every protein, we fit the spectrum and obtain the value of ζ. Notably, the magnitude of ζ correlates with the functional sensitivity and mutational robustness of proteins. As shown in Fig. 3A, as ζ increases, the functional sensitivity described by $1/(\lambda_1\lambda_2)$ decreases. As shown in Fig. 3B, the mutational robustness described by $|\lambda_1^{-1} - \lambda_2^{-1}|$ also decreases as ζ increases. Since both functional sensitivity and mutational robustness are negatively correlated with the coefficient ζ, as shown in Fig. 3C, for proteins with a given size, functional sensitivity is positively correlated with mutational robustness. This behavior resembles that of the three-bead system, as discussed in previous sections, which suggests the low-dimensionality of the dynamics of natural proteins.

The coefficient ζ is closely related to the protein structure. As shown in Fig. 3D, the radius of gyration R_g is negatively correlated with ζ. The three proteins illustrated in Fig. 2D can also support such an analysis. They have the same chain length, but their R_g and ζ are different. The chain length N per volume ($\sim N/R_g^3$) can act as an estimator of the packing density of proteins. A smaller R_g (larger ζ) indicates a higher packing density and lower flexibility of the molecule. On the contrary, a larger R_g (smaller ζ) implies a lower packing density and higher flexibility. The coefficient ζ is correlated with the fractal dimensions of proteins. When a protein is packed in lower spatial dimensions, there will be a smaller ζ and a larger R_g. Besides, there will be a larger solvent-accessible surface area (SASA) [58] and higher modularity [59, 60], contributing to the large-scale motions and slow relaxations of the proteins (see SM).

For natural proteins, both functional sensitivity and mutational robustness are scaled up as the protein size increases. As shown in Fig. 3E, as the chain length N increases, the magnitude of $1/(\lambda_1\lambda_2)$ also increases, showing that large proteins also have a higher functional sensitivity. The physical picture of this relationship is clear: small proteins tend to have a densely packed structure that ensures a stable folded state; while for large proteins, slower vibration modes, which usually correspond with disordered loops or linkers, are demanded by the functionality. Meanwhile, as shown in Fig. 3F, as the protein size increases, the eigengap $|\lambda_1^{-1} - \lambda_2^{-1}|$ also increases, showing that slow vibration modes also exhibit a high mutational robustness. It is also understood that large proteins or protein complexes usually have multi-domain structures, which shows the high modularity of their residue contact networks [8]. The enhancement of the molecular flexibility contributes to inter-domain motions, which are usually highly robust. In all, the size dependence of functional sensitivity and mutational robustness suggests a general evolutionary constraint for proteins with different sizes.

V. DISCUSSIONS

Plasticity and robustness are considered to be the two basic characteristics of biological systems [20–23]. They seem to be two opposite concepts at a first glance; however, proteins can exhibit both the two characteristics. Native proteins are not only robust enough to tolerate random mutations, but also susceptible enough to sense environmental signals and perform large-scale conformational changes. It is suggested that a hidden link evolves between sensitivity/robustness to external perturbations and to mutations [22]. To reveal the relationship between functional sensitivity and mutational robustness, in this study, a general framework is presented to analyze the dynamics of a system under external and internal perturbations.

We demonstrate that for systems with low degrees

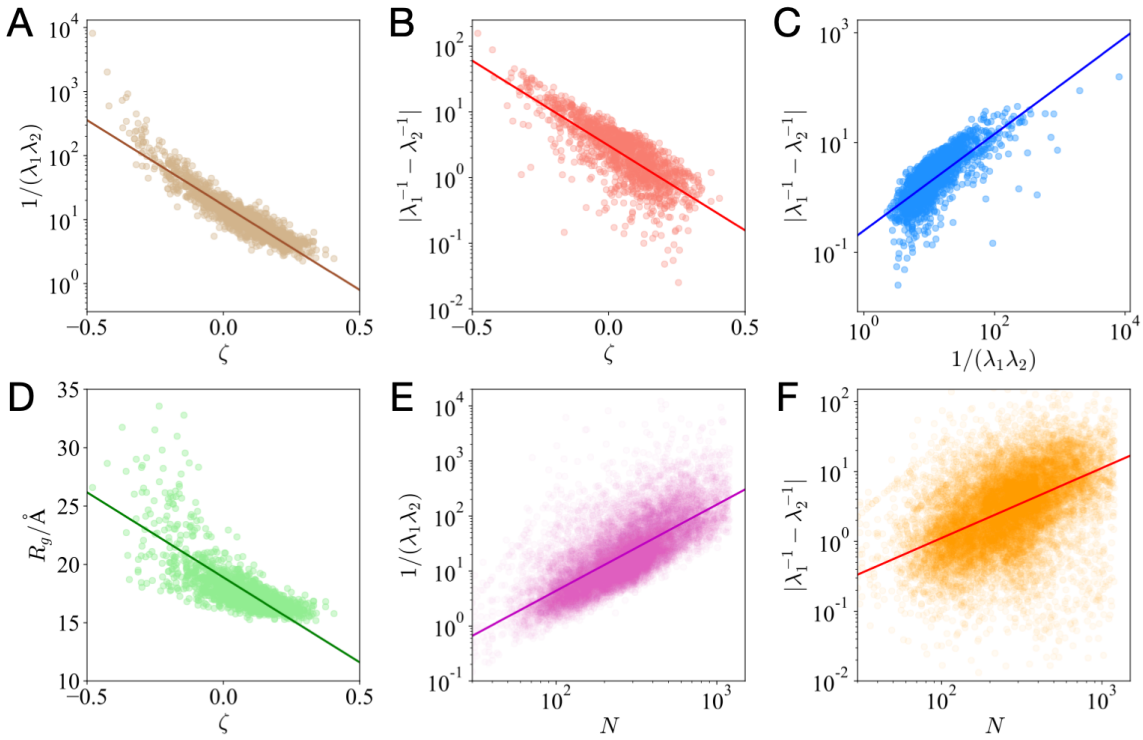

FIG. 3. For proteins with similar sizes (chain length $180 \leq N < 220$), the scattering plots (every data point denotes a protein) and trend lines of (A) functional sensitivity $1/(\lambda_1\lambda_2)$ vs the power-law coefficient ζ; (B) mutational robustness $|\lambda_1^{-1}-\lambda_2^{-1}|$ vs ζ; (C) mutational robustness $|\lambda_1^{-1}-\lambda_2^{-1}|$ vs functional sensitivity $1/(\lambda_1\lambda_2)$; and (D) radius of gyration R_g vs ζ. For proteins with different sizes ($30 \leq N \leq 1200$), the scattering plots (every data point denotes for a protein) and trend lines of (E) functional sensitivity $1/(\lambda_1\lambda_2)$ vs chain length N, and (F) mutational robustness $|\lambda_1^{-1}-\lambda_2^{-1}|$ vs chain length N are shown.

of freedom, high functional sensitivity is equivalent to high mutational robustness. Biological systems, however, involve high degrees of freedom. Here, we show that these degrees of freedom are hierarchically organized, with power-law statistics of eigenvalues of relaxation dynamics. Larger conformational changes are governed by low-dimensional slow modes. Recent reports have shown that the dimensions of biologically relevant modes are reduced through evolution [61, 62]. Such evolutionary dimensional reduction was also observed in the phenotypic dynamics of proteins [27, 28, 63]. Such a property also concerns with "sloppiness" [64–66]. Systems are usually sensitive to perturbations along a few stiff dimensions that correspond with the functional dynamics and highly robust to mutations along many other sloppy dimensions. Both functional sensitivity and mutational robustness can be achieved with these sloppy systems.

The low-dimensional dynamics have a slower timescale in general. These slow-mode motions usually overlap significantly with displacement during functional motions. These functional motions usually involve relative movements of large protein subunits or cooperative conformational changes in entire proteins. They confer a high functional sensitivity; a small perturbation can lead to motions along the directions of these modes. Previous research has shown that weak interactions at the interfaces of domains enable proteins to exhibit large-amplitude conformational changes [67–69], contributing to the functional sensitivity of the molecule. Meanwhile, these functional slow modes are also highly robust to mutations. Modularized structures in residue contact networks define gaps between the eigenvalues of the graph Laplacian [59, 60, 70], and contribute to mutational robustness (details in SM). In practice, the gap between the first and second eigenvalues ($|\lambda_1^{-1}-\lambda_2^{-1}|$ or $\log(\lambda_2/\lambda_1)$) has been applied as an empirical descriptor of protein fitness [27, 28]. One theoretical interpretation is that when protein dynamics are low-dimensional, the maximization of the gap between the first two non-zero eigenvalues can contribute to the functional sensitivity and mutational robustness of a protein molecule.

For systems with high degrees of freedom, our results show that the compatibility between functional sensitivity and mutational robustness will lead to a power-law eigenvalue distribution in the spectrum, which is a sign of criticality. Our statistics for natural proteins reveal that small proteins prefer a densely packed structure to ensure a stable folded state, while large proteins have higher flexibility, which is required for their functionality. Such results reveal a universal principle in the evolution of proteins with different sizes and shed light on the design of functional proteins. Interestingly, staying at the

critical point seems to be a common organizing principle of numerous varieties of biological systems [71–76]: If a system is too disordered, it cannot stably exist or be reproduce; if it is too ordered, it cannot adapt or respond to environmental perturbations. Our model proposes a general mechanism for evolution towards criticality. Our general formulation to link plasticity-robustness compatibility with the ubiquity of critical states can also be generalized for the analysis of the evolution of other complex systems.

ACKNOWLEDGMENTS

We wish to thank Alexander S. Mikhailov, Holger Flechsig, Atsushi Kamimura, Takyuya U Sato, Lei-Han Tang, and Changsong Zhou for participating in stimulating discussions. This research was partially supported by a Grant-in-Aid for Scientific Research on Innovative Areas (17H06386), from the Ministry of Education, Culture, Sports, Science and Technology of Japan, and a Grant-in-Aid for Scientific Research (A)20H00123 from the Japanese Society for the Promotion of Science.

Appendix A: Dataset

Our dataset contains 12954 proteins selected from the Protein Data Bank (PDB) [77]. The structures of these proteins were all determined via high-resolution X-ray diffraction ($\leq$ 2.0Å). No DNA, RNA, or hybrid structures of proteins are included in the dataset, and the chain lengths are $30 \leq N \leq 1200$. In our protein dataset, every two proteins share less than 30% sequence similarity. The PDB codes of all the proteins in our dataset are listed in the SM.

Appendix B: Correlated Motion

The correlated motion of proteins can be described using the covariance matrix C, in which the matrix element $C_{ij} = \langle \Delta\vec{r_i} \cdot \Delta\vec{r_j} \rangle$ described the correlated motion of native proteins [33–35]. With regard to the properties of Gaussian integrals, the covariance matrix C is proportional to the pseudoinverse of the Hessian matrix $\mathcal{H}$: $C \sim \mathcal{H}^{\dagger} = \sum_{i=1}^{N-1} \lambda_i^{-1} \vec{v}_i \vec{v}_i^T$ [17, 24, 31].

Appendix C: Graph Laplacian

In the GNM [31, 32], the Hessian matrix $\mathcal{H}$ is reduced into a Kirchhoff matrix that described residue contact topology. The entries in matrix $\mathcal{H}$ are calculated as:

$$h_{ij} = \begin{cases} -1 & \text{if } i \neq j \text{ and } r_{ij} \leq r_C, \\ 0 & \text{if } i \neq j \text{ and } r_{ij} > r_C, \\ -\sum_{j,j\neq i}^{N} h_{ij} & \text{if } i = j. \end{cases} \tag{C1}$$

Here, r_C is the cut-off distance, and the interaction strength between residues can only be 0 or 1. In this study, we used $r_C = 8.0$Å. Note that the matrix $\mathcal{H}$ can be expressed as $\mathcal{H} = \mathcal{D} - \mathcal{A}$, in which $\mathcal{D}$ is a diagonal matrix that describes the degrees of the nodes, and $\mathcal{A}$ is the adjacency matrix of the elastic network. For the matrix $\mathcal{H}$, the trace $\sum_i \mathcal{H}_{ii} = \sum_i \lambda_i = 2E$, in which E denotes the total number of edges in the elastic network. In a protein molecule, the number of edges, i.e. E indicates the total number of covalent and non-covalent residue contacts. Thus, E can work as an estimator of the energy of the native state.

[1] H. J. Berendsen and S. Hayward, Collective protein dynamics in relation to function, Current opinion in structural biology **10**, 165 (2000).
[2] J. Lippincott-Schwartz, E. Snapp, and A. Kenworthy, Studying protein dynamics in living cells, Nature Reviews Molecular Cell Biology **2**, 444 (2001).
[3] M. Karplus and J. A. McCammon, Molecular dynamics simulations of biomolecules, Nature Structural Biology **9**, 646 (2002).
[4] H. N. Motlagh, J. O. Wrabl, J. Li, and V. J. Hilser, The ensemble nature of allostery, Nature **508**, 331 (2014).
[5] S.-R. Tzeng and C. G. Kalodimos, Dynamic activation of an allosteric regulatory protein, Nature **462**, 368 (2009).
[6] B. J. Grant, A. A. Gorfe, and J. A. McCammon, Large conformational changes in proteins: signaling and other functions, Current Opinion in Structural Biology **20**, 142 (2010).
[7] Q.-Y. Tang, Y.-Y. Zhang, J. Wang, W. Wang, and D. R. Chialvo, Critical fluctuations in the native state of proteins, Physical Review Letters **118**, 088102 (2017).
[8] Q.-Y. Tang and K. Kaneko, Long-range correlation in protein dynamics: Confirmation by structural data and normal mode analysis, PLoS Computational Biology **16**, e1007670 (2020).
[9] E. Marcos, R. Crehuet, and I. Bahar, On the conservation of the slow conformational dynamics within the amino acid kinase family: Nagk the paradigm, PLoS Computational Biology **6**, e1000738 (2010).
[10] L. Ponzoni and I. Bahar, Structural dynamics is a determinant of the functional significance of missense variants, Proceedings of the National Academy of Sciences **115**, 4164 (2018).
[11] H. H. Guo, J. Choe, and L. A. Loeb, Protein tolerance to random amino acid change, Proceedings of the National Academy of Sciences **101**, 9205 (2004).
[12] N. Tokuriki and D. S. Tawfik, Stability effects of mutations and protein evolvability, Current opinion in structural biology **19**, 596 (2009).
[13] M. Soskine and D. S. Tawfik, Mutational effects and the evolution of new protein functions, Nature Reviews Ge-

netics **11**, 572 (2010).
[14] E. Shakhnovich, Protein folding thermodynamics and dynamics: where physics, chemistry, and biology meet, Chemical Reviews **106**, 1559 (2006).
[15] J. K. Weber and V. S. Pande, Protein folding is mechanistically robust, Biophysical Journal **102**, 859 (2012).
[16] W. Zheng, B. R. Brooks, and D. Thirumalai, Low-frequency normal modes that describe allosteric transitions in biological nanomachines are robust to sequence variations, Proceedings of the National Academy of Sciences **103**, 7664 (2006).
[17] I. Bahar, T. R. Lezon, L.-W. Yang, and E. Eyal, Global dynamics of proteins: bridging between structure and function, Annual Review of Biophysics **39**, 23 (2010).
[18] I. Bahar, M. H. Cheng, J. Y. Lee, C. Kaya, and S. Zhang, Structure-encoded global motions and their role in mediating protein-substrate interactions, Biophysical journal **109**, 1101 (2015).
[19] T. Haliloglu and I. Bahar, Adaptability of protein structures to enable functional interactions and evolutionary implications, Current opinion in structural biology **35**, 17 (2015).
[20] A. Wagner, *Robustness and Evolvability in Living Systems* (Princeton University Press, 2007).
[21] K. Kaneko, Relationship among phenotypic plasticity, phenotypic fluctuations, robustness, and evolvability; waddington's legacy revisited under the spirit of einstein, Journal of Biosciences **34**, 529 (2009).
[22] K. Kaneko, Evolution of robustness and plasticity under environmental fluctuation: Formulation in terms of phenotypic variances, Journal of Statistical Physics **148**, 687 (2012).
[23] T. S. Hatakeyama and K. Kaneko, Reciprocity between robustness of period and plasticity of phase in biological clocks, Physical Review Letters **115**, 218101 (2015).
[24] M. M. Tirion, Large amplitude elastic motions in proteins from a single-parameter, atomic analysis, Physical Review Letters **77**, 1905 (1996).
[25] C. Chennubhotla, A. Rader, L.-W. Yang, and I. Bahar, Elastic network models for understanding biomolecular machinery: from enzymes to supramolecular assemblies, Physical Biology **2**, S173 (2005).
[26] W. Zheng and S. Doniach, A comparative study of motor-protein motions by using a simple elastic-network model, Proceedings of the National Academy of Sciences **100**, 13253 (2003).
[27] H. Flechsig and Y. Togashi, Designed elastic networks: Models of complex protein machinery, International Journal of Molecular Sciences **19**, 3152 (2018).
[28] J.-P. Eckmann, J. Rougemont, and T. Tlusty, Colloquium: Proteins: The physics of amorphous evolving matter, Reviews of Modern Physics **91**, 031001 (2019).
[29] O. Rivoire, Parsimonious evolutionary scenario for the origin of allostery and coevolution patterns in proteins, Physical Review E **100**, 032411 (2019).
[30] K. Husain and A. Murugan, Physical constraints on epistasis, arXiv (2019).
[31] T. Haliloglu, I. Bahar, and B. Erman, Gaussian dynamics of folded proteins, Physical Review Letters **79**, 3090 (1997).
[32] T. Haliloglu and B. Erman, Analysis of correlations between energy and residue fluctuations in native proteins and determination of specific sites for binding, Physical Review Letters **102**, 088103 (2009).
[33] D. A. Case, Normal mode analysis of protein dynamics, Current Opinion in Structural Biology **4**, 285 (1994).
[34] V. Alexandrov, U. Lehnert, N. Echols, D. Milburn, D. Engelman, and M. Gerstein, Normal modes for predicting protein motions: a comprehensive database assessment and associated web tool, Protein Science **14**, 633 (2005).
[35] H. Wako and S. Endo, Normal mode analysis as a method to derive protein dynamics information from the protein data bank, Biophysical Reviews **9**, 877 (2017).
[36] M. Ikeguchi, J. Ueno, M. Sato, and A. Kidera, Protein structural change upon ligand binding: linear response theory, Physical Review Letters **94**, 078102 (2005).
[37] P. Das, M. Moll, H. Stamati, L. E. Kavraki, and C. Clementi, Low-dimensional, free-energy landscapes of protein-folding reactions by nonlinear dimensionality reduction, Proceedings of the National Academy of Sciences **103**, 9885 (2006).
[38] E. Papaleo, P. Mereghetti, P. Fantucci, R. Grandori, and L. De Gioia, Free-energy landscape, principal component analysis, and structural clustering to identify representative conformations from molecular dynamics simulations: the myoglobin case, Journal of Molecular Graphics and Modelling **27**, 889 (2009).
[39] F. Sittel and G. Stock, Perspective: Identification of collective variables and metastable states of protein dynamics, The Journal of Chemical Physics **149**, 150901 (2018).
[40] I. Bahar, On the functional significance of soft modes predicted by coarse-grained models for membrane proteins, Journal of General Physiology **135**, 563 (2010).
[41] V. Hnizdo and M. K. Gilson, Thermodynamic and differential entropy under a change of variables, Entropy **12**, 578 (2010).
[42] A. T. Fenley, B. J. Killian, V. Hnizdo, A. Fedorowicz, D. S. Sharp, and M. K. Gilson, Correlation as a determinant of configurational entropy in supramolecular and protein systems, The Journal of Physical Chemistry B **118**, 6447 (2014).
[43] J. Numata, M. Wan, and E.-W. Knapp, Conformational entropy of biomolecules: beyond the quasi-harmonic approximation, Genome Informatics **18**, 192 (2007).
[44] T. Greville, Some applications of the pseudoinverse of a matrix, SIAM Review **2**, 15 (1960).
[45] V. Frappier, M. Chartier, and R. J. Najmanovich, Encom server: exploring protein conformational space and the effect of mutations on protein function and stability, Nucleic acids research **43**, W395 (2015).
[46] C. H. Rodrigues, D. E. Pires, and D. B. Ascher, Dynamut: predicting the impact of mutations on protein conformation, flexibility and stability, Nucleic acids research **46**, W350 (2018).
[47] T. Kato, *Perturbation theory for linear operators (2nd ed.)* (Springer-Verlag Berlin Heidelberg, 1995).
[48] O. Sporns and R. F. Betzel, Modular brain networks, Annual Review of Psychology **67**, 613 (2016).
[49] E. T. Jaynes, Information theory and statistical mechanics, Physical Review **106**, 620 (1957).
[50] T. Mora, A. M. Walczak, W. Bialek, and C. G. Callan, Maximum entropy models for antibody diversity, Proceedings of the National Academy of Sciences **107**, 5405 (2010).
[51] T. R. Lezon and I. Bahar, Using entropy maximization to understand the determinants of structural dynamics beyond native contact topology, PLoS Computational Bi-

ology **6**, e1000816 (2010).
[52] F. Seno, A. Trovato, J. R. Banavar, and A. Maritan, Maximum entropy approach for deducing amino acid interactions in proteins, Physical Review Letters **100**, 078102 (2008).
[53] T. X. Hoang, F. Seno, A. Trovato, J. R. Banavar, and A. Maritan, Inference of the solvation energy parameters of amino acids using maximum entropy approach, The Journal of chemical physics **129**, 07B613 (2008).
[54] S. Reuveni, R. Granek, and J. Klafter, Proteins: coexistence of stability and flexibility, Physical Review Letters **100**, 208101 (2008).
[55] P. Erdős and A. Rényi, On the evolution of random graphs, Publ. Math. Inst. Hung. Acad. Sci **5**, 17 (1960).
[56] M. Penrose, *Random geometric graphs* (Oxford university press, 2003).
[57] A. Arenas, A. Díaz-Guilera, and C. J. Pérez-Vicente, Synchronization reveals topological scales in complex networks, Physical Review Letters **96**, 114102 (2006).
[58] M. L. Connolly, Solvent-accessible surfaces of proteins and nucleic acids, Science **221**, 709 (1983).
[59] M. E. Newman and M. Girvan, Finding and evaluating community structure in networks, Physical Review E **69**, 026113 (2004).
[60] M. E. Newman, Modularity and community structure in networks, Proceedings of the national academy of sciences **103**, 8577 (2006).
[61] K. Kaneko and C. Furusawa, Macroscopic theory for evolving biological systems akin to thermodynamics, Annual Review of Biophysics **47**, 273 (2018).
[62] T. U. Sato and K. Kaneko, Evolutionary dimension reduction in phenotypic space, Physical Review Research **2**, 013197 (2020).
[63] S. Dutta, J.-P. Eckmann, A. Libchaber, and T. Tlusty, Green function of correlated genes in a minimal mechanical model of protein evolution, Proceedings of the National Academy of Sciences **115**, E4559 (2018).
[64] R. N. Gutenkunst, J. J. Waterfall, F. P. Casey, K. S. Brown, C. R. Myers, and J. P. Sethna, Universally sloppy parameter sensitivities in systems biology models, PLoS Computational Biology **3**, e0030189 (2007).
[65] B. C. Daniels, Y.-J. Chen, J. P. Sethna, R. N. Gutenkunst, and C. R. Myers, Sloppiness, robustness, and evolvability in systems biology, Current opinion in biotechnology **19**, 389 (2008).
[66] M. K. Transtrum, B. B. Machta, K. S. Brown, B. C. Daniels, C. R. Myers, and J. P. Sethna, Perspective: Sloppiness and emergent theories in physics, biology, and beyond, The Journal of chemical physics **143**, 07B201_1 (2015).
[67] J. Siltberg-Liberles, J. A. Grahnen, and D. A. Liberles, The evolution of protein structures and structural ensembles under functional constraint, Genes **2**, 748 (2011).
[68] S. Pechmann, E. D. Levy, G. G. Tartaglia, and M. Vendruscolo, Physicochemical principles that regulate the competition between functional and dysfunctional association of proteins, Proceedings of the National Academy of Sciences **106**, 10159 (2009).
[69] W. Li, P. G. Wolynes, and S. Takada, Frustration, specific sequence dependence, and nonlinearity in large-amplitude fluctuations of allosteric proteins, Proceedings of the National Academy of Sciences **108**, 3504 (2011).
[70] A. Pothen, H. D. Simon, and K.-P. Liou, Partitioning sparse matrices with eigenvectors of graphs, SIAM Journal on Matrix Analysis and Applications **11**, 430 (1990).
[71] T. Mora and W. Bialek, Are biological systems poised at criticality?, Journal of Statistical Physics **144**, 268 (2011).
[72] A. R. Honerkamp-Smith, S. L. Veatch, and S. L. Keller, An introduction to critical points for biophysicists; observations of compositional heterogeneity in lipid membranes, Biochimica et Biophysica Acta (BBA)-Biomembranes **1788**, 53 (2009).
[73] D. R. Chialvo, Emergent complex neural dynamics, Nature physics **6**, 744 (2010).
[74] C. Furusawa and K. Kaneko, Zipfś law in gene expression, Physical Review Letters **90**, 088102 (2003).
[75] C. Furusawa and K. Kaneko, Adaptation to optimal cell growth through self-organized criticality, Physical Review Letters **108**, 208103 (2012).
[76] M. A. Munoz, Colloquium: Criticality and dynamical scaling in living systems, Reviews of Modern Physics **90**, 031001 (2018).
[77] H. M. Berman, J. Westbrook, Z. Feng, G. Gilliland, T. N. Bhat, H. Weissig, I. N. Shindyalov, and P. E. Bourne, The protein data bank, Nucleic acids research **28**, 235 (2000).

Supplementary Materials of

Functional Sensitivity and Mutational Robustness of Proteins

Qian-Yuan Tang, Tetsuhiro S. Hatakeyama, Kunihiko Kaneko

1 Functional Sensitivity and Condition Number

In numerical computations, the condition number is usually introduced to measure the sensitivity of a function, say, how much would the errors or perturbations in the input lead to the error in the output. In this work, based on the Gaussian network model (GNM), the protein molecules are simplified as linear systems. Then, we can define a condition number to measure the sensitivity of a protein molecule. Such a definition is consistent with the fluctuation entropy as defined in the main text.

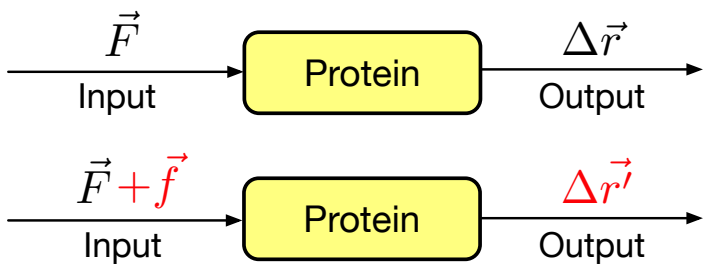

Figure S1: A protein molecule is modelled as a linear system. With the external force $\vec{F}$ as the input, the molecule would have deformation $\Delta\vec{r}$ as the output. When input arguments $\vec{f}$ is added to the molecule, then the output is modified as $\Delta\vec{r'}$.

Here, as shown in Fig. S1, we take external force $\vec{F}$ (such as protein hydration, ligand binding, protein-protein interactions, or other perturbations from the environment) as the input, and take the molecular deformation $\Delta\vec{r}$ from the native state (molecular vibrations or conformational changes) as the output. In the linear regime, the relationship between the output $\Delta\vec{r}$ and the input $\vec{F}$ would be: $\vec{\Delta r} = \mathcal{H}^{\dagger}\vec{F}$, where $\mathcal{H}^{\dagger}$ denotes the pseudoinverse of the Hessian matrix $\mathcal{H}$. In a fluctuating environment, when external perturbations (input arguments) $\vec{f}$ act on the molecule, the deformation (output errors) of the molecule changes from $\Delta\vec{r}$ to $\Delta\vec{r'}$. The relative change in the deformation (output) would be $||\Delta\vec{r'}-\Delta\vec{r}||/||\Delta\vec{r}||$ and the relative change in the external force (input) would be $||\vec{f}||/||\vec{F}||$. The ratio of the relative output ($\Delta\vec{r}$) error versus relative input ($\vec{F}$) error

$$c = \frac{\frac{||\Delta\vec{r'}-\Delta\vec{r}||}{||\Delta\vec{r}||}}{\frac{||\vec{f}||}{||\vec{F}||}} = \frac{||\mathcal{H}^{\dagger}\vec{f}||}{||\mathcal{H}^{\dagger}\vec{F}||}\cdot\frac{||\vec{F}||}{||\vec{f}||} \tag{S1}$$

We define sensitivity of a protein molecule as the maximum value c^* of the ratio c, which is given by

$$c^* = \frac{\max||\mathcal{H}^{\dagger}\vec{f}||\cdot||\vec{F}||}{\min||\mathcal{H}^{\dagger}\vec{F}||\cdot||\vec{F}||} = \frac{\lambda_{\max}}{\lambda_{\min}} = \frac{\lambda_{N-1}}{\lambda_1}. \tag{S2}$$

The value of c^* describes how much would the perturbations in external forces lead to the changes in the deformation of a protein molecule. Note that the value c^* can be understood as a generalization of condition number, which is widely applied in the measurement of the intrinsic sensitivity of linearized dynamics. An ill-conditioned protein molecule can exhibit large conformational changes with low energy costs, which is highly beneficial in performing its functional dynamics. An ill-conditioned network structure corresponds to a protein molecule shows high sensitivity under external perturbations.

Note that the condition number c^* has its limitations: the optimization towards the maximum condition number can only affect the largest and the smallest eigenvalue. Therefore, in the Main Text, we introduce fluctuation entropy to quantify the functional sensitivity of the molecule. According to Eq.(3) in the main text, the fluctuation entropy S_F is a convex function of eigenvalue λ_j's. When we fix the total number of contact (total number of edges) as E, the fluctuation entropy S_F and the condition number c^* will be two correlated descriptors of sensitivity: according to Jensen's inequality, the fluctuation entropy reaches the minimum when all the eigenvalues take the same value. In such a situation, the condition number c^* also reaches minimum ($c^* = 1$). The fluctuation entropy reaches maximum when the first $N-2$ vibration modes have the corresponding eigenvalues that ($\lambda_1 \approx \lambda_2 \approx \cdots \approx \lambda_{N-2} \approx 0$) and the fastest mode correspond to $\lambda_{N-1} \approx 2E$. In such a situation, the condition number $c^* \to \infty$.

2 Mutational Robustness based on the Intersection Angle

In the Main Text, to quantify the mutational robustness of the j-th eigenvector $\vec{v}_j$, we introduced the square deviation $|\Delta\vec{v}_j|^2$ to measure the "distance" from the original $\vec{v}_j$ to $\vec{v}'_j$. Another way to quantify the robustness of an eigenvector is to estimate the intersection angle $\langle\vec{v}_j, \vec{v}'_j\rangle$ between the unperturbed and perturbed eigenvectors. It is worth noting that, with other definitions of the "distance" between two eigenvectors, our analysis for the mutational robustness of a given eigenvector can also hold. For simplification, in the following discussions, we omit the notations of vectors and write $\vec{v}_j$ as v_j.

2.1 Mutational robustness based on the intersection angle

When a mutation happens on site p, the Hessian matrix then changes from $\mathcal{H}$ to $\mathcal{H}'$, where $\mathcal{H}' = \mathcal{H} + \epsilon M$. According to Davis-Kahan Theorem [1, 2], the difference between the unperturbed eigenvector v_j and the perturbed v'_j

$$\sin\langle v_j, v'_j\rangle \leq \frac{2 \cdot \epsilon ||M||_{\text{op}}}{\min(\lambda_{j+1} - \lambda_j, \lambda_j - \lambda_{j-1})}, \tag{S3}$$

in which $||M||_{\text{op}}$ is the operator norm of matrix M, which is defined as the largest singular value of matrix.

As shown in Eq.S3, the robustness of the j-th eigenvector is determined by the magnitude of the perturbation ϵ, the operator norm $||M||_{\text{op}}$ and the minimum gap between neighboring eigenvalues. Here, the magnitude of perturbation ϵ can be recognized as a constant, and for adding or removing a contact, there will be $||M||_{\text{op}} = 1$. In such a situation, the robustness of the eigenvector v_j is only determined by the gaps between the neighboring eigenvalues $\lambda_j - \lambda_{j-1}$ and $\lambda_{j+1} - \lambda_j$. Such a result is also in line with the classical perturbation theory as discussed in the Main Text.

2.2 The inverse of the eigenvalues

For the low-frequency modes with $\lambda_i \approx 0$, the eigengaps $|\lambda_i - \lambda_{i-1}|$ are too small, according to Davis-Kahan theorem, there will always be a very high upper bound for the intersection angle. To have an accurate estimation of the mutational robustness, one shall use the eigengaps in the psedudoinverse of the matrix $\mathcal{H}$ (which is proportional to covariance matrix) to estimate how much would such a mutation affect the covariance matrix C ($\sim \mathcal{H}^\dagger$). We have

$$\begin{aligned}(\mathcal{H}')^\dagger &= \Big(\mathcal{H}(I + \epsilon\mathcal{H}^\dagger M)\Big)^\dagger = (I + \epsilon\mathcal{H}^\dagger N)^\dagger \cdot \mathcal{H}^\dagger \\ &\approx \mathcal{H}^\dagger - \epsilon\mathcal{H}^\dagger M\mathcal{H}^\dagger. \end{aligned} \tag{S4}$$

Then, according to Davis-Kahan theorem, we have

$$\sin\langle v_j, v_j'\rangle \leq \frac{2 \cdot \epsilon ||\mathcal{H}^\dagger M\mathcal{H}^\dagger||_{\text{op}}}{\min(\lambda_{j+1}^{-1} - \lambda_j^{-1}, \lambda_j^{-1} - \lambda_{j-1}^{-1})}. \tag{S5}$$

Eq.S5 shows that the mutational robustness of v_j is bounded by the eigengaps in the $\mathcal{H}^\dagger$. Therefore in the Main Text, we introduce $|\lambda_1^{-1} - \lambda_2^{-1}|$ to describe the robustness of the v_1.

2.3 Distance between linear subspaces

The Davis–Kahan theorem can also be used in the perturbation analysis to bound the distance between linear subspaces. As discussed in Ref. [2], for $N \times N$ symmetric real matrix A and $\hat{A}$, let us consider the distance between the two subspace $V = (v_r, v_{r+1}, \cdots, v_s) \in \mathbb{R}^{N\times d}$ and $\hat{V} = (\hat{v}_r, \hat{v}_{r+1}, \cdots, \hat{v}_s) \in \mathbb{R}^{N\times d}$ $(1 \leq r \leq s \leq N)$.

To calculate the "distance" between the two subspace, we compare the difference in the principal angles between the two subspace. To determine the angle, we calculate the inner product of the two subspaces $\hat{V}^T V$, and there are d singular values $(\sigma_1, \sigma_2, \cdots \sigma_d)$ for matrix $\hat{V}^T V$. Since both V and $\hat{V}$ have orthonormal columns, these singular values reflect the d principal angles between their column spaces, which are given by $\cos^{-1}\sigma_1, \cos^{-1}\sigma_2, \cdots \cos^{-1}\sigma_d$. Then, we define the $\Theta(V, \hat{V})$ as a $d \times d$ diagonal matrix in which $\Theta_{jj} = \cos^{-1}\sigma_j$, and $1 \leq j \leq N$.

According to the useful variant of the Davis-Kahan theorem [2], the distance $\Theta(V, \hat{V})$ between the two $d-$dimensional subspace V and $\hat{V}$ would be bounded as:

$$||\sin\Theta(\hat{V}, V)||_{\text{F}} \leq \frac{2 \cdot \min(d^{1/2}||\hat{A} - A||_{\text{op}}, ||\hat{A} - A||_{\text{F}})}{\min(\lambda_{r-1} - \lambda_r, \lambda_s - \lambda_{s+1})}, \tag{S6}$$

in which $||\cdot||_F$ is the Frobenius Norm of the matrix, which is defined as $||A||_{\text{F}} = \sqrt{\text{Tr}(A^T A)} = \sqrt{\sum_{i=1}^M \sum_{j=1}^N |a_{ij}|^2} = \sqrt{\sum_{i=1}^r \sigma_i^2}$. Eq.S6 shows that the robustness of the eigenvectors against matrix element perturbation is determined by the eigengaps of the matrix. For every eigenvalue λ_j of matrix A, there are two eigengaps: $\lambda_{j-1} - \lambda_j$ and $\lambda_j - \lambda_{j+1}$ (For $j = 1$, here we define $\lambda_0 = -\infty$, and for $j = N$, we define $\lambda_{N+1} = \infty$.) These eigengaps work as the intrinsic attributes which determine the robustness of a matrix under perturbation. As illustrated in Fig.S2, the distance between the perturbed and unperturbed subspace is bounded by the eigengaps at the boundary of the (unperturbed) subspace.

We can also define the distance between two linear spaces based on the Chebyshev distance. In mathematics, the Chebyshev distance between two vectors is defined as the maximum of their differences along any coordinate dimension. Therefore, such a metric is also called the "maximum metric". One can also generalize such a metric to quantify the distance between two matrices (linear space) V and $\hat{V}$, that is, the distance between two matrices

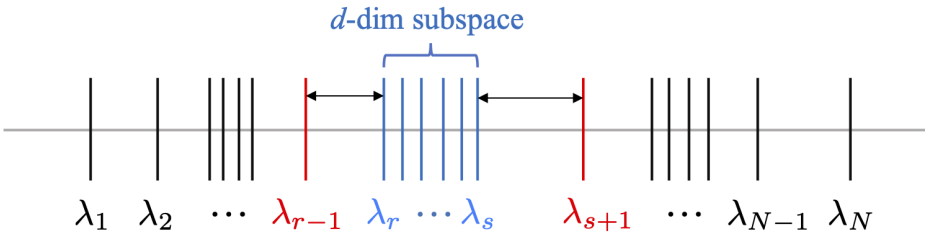

Figure S2: The robustness of the subspace is determined by the eigengaps. The distance between the perturbed and unperturbed subspace can be determined by the eigengaps at the boundary of the subspace.

is defined as the maximum of their differences along any column (the eigenvector with the same ordinal value). Such a metric is intuitive, to measure the distance between two linear spaces, one should first determine which column has changed the most, and then measure how much it changes for such a column. With such a metric, the distance between two eigenspaces is defined as the maximum distance between the eigenvectors (or columns) with the same ordinal value from the two eigenspaces.

Then, one can define the maximum Euclidean distance between the two eigenspaces as

$$\max_{1\leq i\leq d} ||\hat{v}_i - v_i||_2,$$

that is, the distance between two eigenspaces is defined as the maximum Euclidean distance between the two eigenvectors with the same ordinal value from the two eigenspaces.

Or one can define the maximum Chebyshev distance between the two eigenspaces as

$$\max_{1\leq i\leq d}\left(\max_{1\leq j\leq N} |\hat{v}_{ij} - v_{ij}|\right),$$

that is, the distance between two eigenspaces is defined as the maximum Chebyshev distance between the two eigenvectors with the same ordinal value from the two eigenspaces.

In brief, for the eigenspace which has larger eigengaps between neighboring eigenvalues, such an eigenspace would be more robust under perturbation. Therefore, to maximize the robustness of the eigenspace, one should maximize the minimum eigengap between neighboring eigenvalues.

2.4 Uniform eigenvalue distribution relates to the highest eigenspace robustness

In this subsection, we prove that, when the magnitude of the perturbation (the norm of the perturbation matrix) is fixed, a uniform eigenvalue distribution gives the highest eigenspace robustness. Consider the eigenspace $V = (v_1, v_2, v_3, \cdots, v_d) \in \mathbb{R}^{N\times d}$ correspond with non-negative eigenvalues $\{\lambda_1, \lambda_2, \lambda_3, \cdots \lambda_d\}$, and $0 \leq \lambda_1 \leq \lambda_2 \leq \lambda_3 \leq \cdots \leq \lambda_d$. With a fixed summation of eigenvalues (i.e., fix $\sum_i \lambda_i = S > 0$), to maximize the minimum eigengaps $g_{\min}$, the spectrum $\{\lambda_1, \lambda_2, \lambda_3, \cdots \lambda_d\}$ should be an arithmetic series, $\lambda_1 = 0$ with a constant difference, i.e., $\lambda_i = c(i-1)$ with $c = \frac{2s}{d(d-1)}$.

Assume that there is a non-negative sequence $\{\lambda'_1, \lambda'_2, \lambda'_3, \cdots \lambda'_d\}$ other than the arithmetic series can maximize the minimum eigengaps with fix summation S, and the minimum gap g^* could be found between the j-th and $(j-1)$-th eigenvalue, then we have $\lambda_j - \lambda_{j-1} = g^* > g_{\min}$, and $\lambda_j - \lambda_{j-1} < \lambda_i - \lambda_{i-1}$ for $j \neq i$. In such a situation, the summation of all the eigenvalue

$$S = \sum_{i=1}^{d} \lambda'_i \geq d\lambda'_1 + \frac{d(d-1)g^*}{2} > \frac{d(d-1)g^*}{2} > \frac{d(d-1)g_{\min}}{2} = S,$$

which lead to $S > S$. Therefore, the assumption is not true. Thus, the spectrum which maximizes the minimum eigengaps would be an arithmetic series. In the Main Text, we introduce the Shannon entropy of the spectrum to evaluate the mutational robustness of the system, because the maximum-entropy distribution (without other constraints) would be the uniform distribution that can maximize the minimum gaps between neighboring eigenvalues.

3 Remarks on the Entropy Maximization

3.1 Maximizing fluctuation Entropy

In the Main Text, by taking fluctuation entropy as a constraint, we maximize the spectrum entropy of the system. Similar distribution can also be obtained by taking spectrum entropy as a constraint and maximize the fluctuation entropy. In such an optimization process, there are three constraints:

(a) The spectrum distribution should be normalized, i.e., $\int g(\lambda)d\lambda = 1$;

(b) The total number of contacts in the proteins is a constant, i.e., to fix the trace of the Hessian matrix $\int \lambda g(\lambda)d\lambda = m$;

(c) Robustness constraint: $\int g(\lambda)\log g(\lambda)d\lambda = \mathcal{C}'$.

Take the three constraints as Lagrangian multiplier, then we can obtain the Lagrangian expression:

$$\hat{\mathcal{S}} = -\int \log\lambda \cdot g(\lambda)d\lambda + \eta_0\left(\int g(\lambda)d\lambda - 1\right) + \eta_1\left(\int \lambda g(\lambda)d\lambda - m\right) + \eta\left(\int g(\lambda)\log g(\lambda)d\lambda - \mathcal{C}'\right). \tag{S7}$$

To find the distribution function $g^*(\lambda)$ that maximize entropy $\hat{\mathcal{S}}$ across all probability distributions, we require that:

$$\frac{\partial \hat{S}}{\partial g(\lambda)} = -\log\lambda + \eta_0 + \eta_1\lambda + \eta(\log g(\lambda) + 1) = 0, \tag{S8}$$

hence $g^*(\lambda)$ can be solved as:

$$g^*(\lambda) = e^{-1-\hat{\eta}_0-\hat{\eta}_1\lambda}\lambda^{1/\eta}, \tag{S9}$$

in which $\hat{\eta}_0 = \eta_0/\eta$ and $\hat{\eta}_1 = \eta_1/\eta$. Such a spectrum distribution is also a power-law distribution with an exponential cutoff, which agrees with the form obtained in the Main Text. In the slow-mode limit, the power-law exponent equals $1/\eta$.

3.2 Kullback-Leibler divergence

In the Main Text, we mentioned that the spectrum entropy S can be understood as the Kullback-Leibler divergence from the uniform distribution. Here is the proof.

Suppose $q(x)$ is a uniform distribution ($q(x) = c$ for x defined on the interval X). For a given distribution $p(x)$, to minimize the K-L divergence from $q(x)$ to $p(x)$, we have

$$\begin{aligned} D_{KL}(p||q) &= \int_{x\in X} p(x)\log p(x)dx - \int_{x\in X} p(x)\log q(x)dx \\ &= -S - \int_{x\in X} p(x)\log c dx = -S - \log c \cdot ||X||, \end{aligned} \tag{S10}$$

in which $||X||$ is the measure of interval X, and it is a constant. Thus, minimizing the K-L divergence from given distribution $p(x)$ to uniform distribution $q(x)$ is equivalent with the maximization of spectrum entropy S.

3.3 The eigenvalue distribution and the spectral dimension

In the Main Text, we take three proteins with the same chain length ($N = 200$) as examples to fit the eigenvalue distribution and obtain different values of the power-law coefficient ζ. Here, more proteins are taken for analysis. For proteins with the chain length $N = 200$, the scattering plots of power-law coefficient ζ vs radius of gyration R_g are shown in Fig.S3A. The linear fitting (red line) shows the basic trend of these data: as R_g increases, ζ decreases. To demonstrate the relation between protein structure and the coefficient ζ, among the proteins listed in Fig.S3A, 9 proteins are selected, and their structures are illustrated in Fig.S3B. These proteins have the same chain length ($N = 200$), and they are ordered by their R_g. As shown in Fig.S3B, the protein with a positive ζ and a small R_g usually have more secondary structures and are packed into a globular shape; while those proteins with a negative ζ and a large R_g have more disordered segments or their shape deviate from a globule.

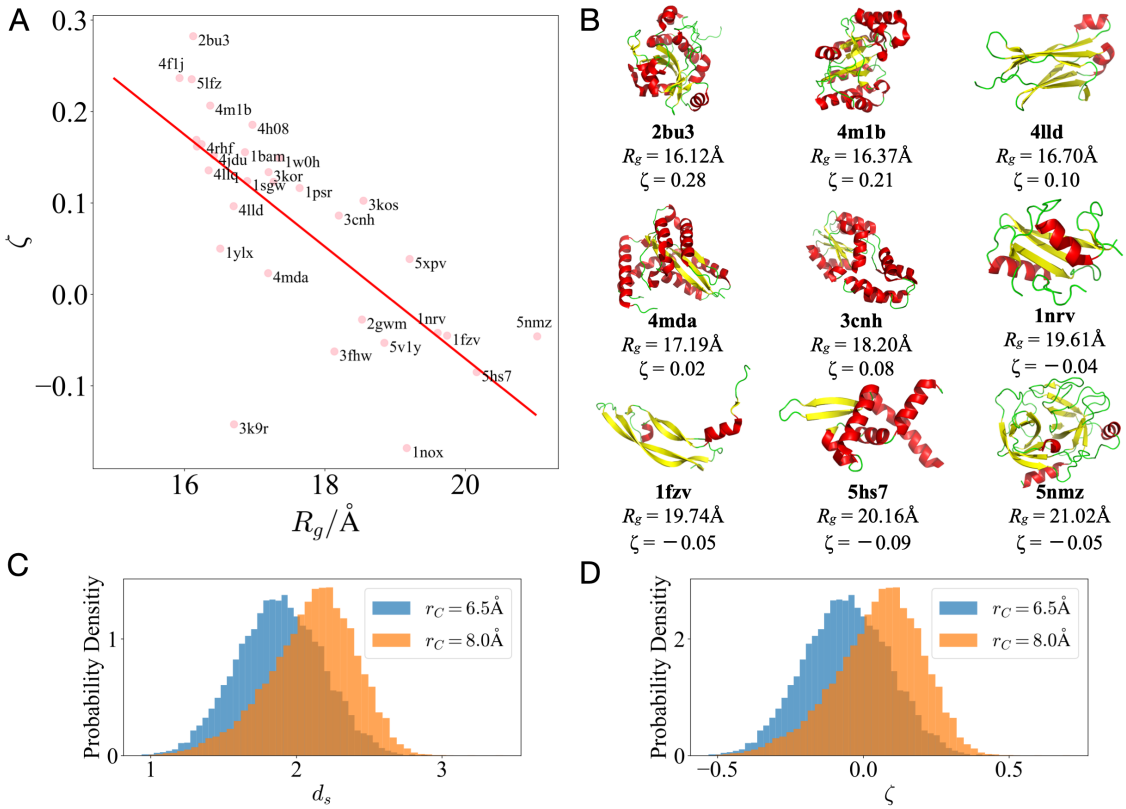

Figure S3: (A) For proteins with the same chain length ($N = 200$), the scattering plots and the linear fit of ζ vs R_g. Every data point denotes a protein. (B) The cartoon structure of 9 proteins with chain length $N = 200$. The PDB code, R_g, and ζ are also listed in the figure. (C) The histogram of the spectral dimension d_s and (D) the histogram of the power-law coefficient ζ for all the proteins in our data set.

The value of ζ is closely related to the spectral dimension d_s of the proteins. The spectral dimension d_s is defined based on the eigenfrequency distribution [3]. In the slow-mode limit, when the eigenfrequency distribution obeys the power law: $f(\omega) \sim \omega^{d_s-1}$, in which d_s denotes the spectral dimension of the protein, the integration of the eigenfrequency distribution $F(\omega) = \int_0^\omega f(\omega')d\omega' = \omega^{d_s}$. Note that in the discrete version, both $F(\omega_i)$ and $G(\lambda_i)$ correspond to the eigenvalue (or eigenfrequency) index i of the system, so $i \sim \omega_i^{d_s} = \lambda_i^{\zeta+1}$. In normal mode analysis, the eigenvalue λ_i is proportional to the square of the eigenfrequency

ω_i^2 [4]. Thus, we have $d_s = 2(\zeta + 1)$. In our work, we take the cutoff distance $r_C = 8.0$Å. In such a situation, the spectral dimension $d_s \approx 2 < 3$, and $\zeta \approx 0$. As shown in Fig. S3C and D, both the spectral dimension d_s and the power-law coefficient ζ are robust for the selection of different parameters (cutoff distance r_C). With a shorter cutoff distance, for example, $r_C = 6.5$Å (as selected in Ref.[3]), there will be a slightly smaller d_s and ζ (because shorter cutoff distances corresponds to more slow modes [5]), but we still have $d_s \approx 2$ and $\zeta \approx 0$.

4 Additional Discussions based on Protein Data

4.1 The size-dependence of functional sensitivity and mutational robustness

In the Main Text, to uncover how the scaling coefficient ζ relates to the functional sensitivity and mutational robustness of a protein, we focus on a subset of proteins with similar chain lengths ($180 \leq N < 220$). The relation between functional sensitivity (or mutational robustness) and ζ also holds for proteins with different sizes. As shown in Fig. S4A, for protein at different sizes, as ζ increases, the functional sensitivity described by $1/(\lambda_1\lambda_2)$ decreases. As shown in Fig. S4B, for protein at different sizes, the mutational robustness described by $|\lambda_1^{-1} - \lambda_2^{-1}|$ also decreases as ζ increases. As shown in Fig. S4C, for protein at different sizes, functional sensitivity is still positively correlated with mutational robustness.

For natural proteins, the mutational robustness increase as the size of the protein increases. In the Main Text, we demonstrate that, as the size of the protein increases, the eigengap $|\lambda_1^{-1} - \lambda_2^{-1}|$ also increases, showing that the slow vibration modes also have high mutational robustness. Here, in Fig. S4D and Fig. S4E, the eigengap $|\lambda_2^{-1} - \lambda_3^{-1}|$ and $|\lambda_3^{-1} - \lambda_4^{-1}|$ also increase as the protein size increases. Such results suggest that, for real proteins, optimizing the mutational robustness of a specific slow mode may also contribute to the mutational robustness of other slow modes.

4.2 The physical meaning of the power-law coefficient

To understand how the power-law coefficient ζ is related to the structure of the proteins, in the Main Text, we introduce the chain length per volume (N/R_g^3) to estimate the packing density of the amino-acid residues and discuss the relationship between the radius of gyration R_g and ζ. With only R_g information, the protein is approximated as a perfect globule, in which all residue interactions are neglected. Such a description oversimplified the structure of the protein. Coefficient ζ can correlate with more detailed information on the structure and dynamics of the proteins.

4.2.1 Solvent-accessible surface area (SASA)

In protein folding, the burial of hydrophobic amino-acid residues is a driving force. The flexibility of the proteins is closely related to the surface area buried within its fold [6]. If proteins are always folded into a perfect globule, the for proteins at similar sizes (similar chain length N), SASA $\sim R_g^2 \sim N^{2/3}$ should be a constant. For real proteins, however, their shape will deviate from the perfect globule and their SASAs also vary. Here, we focus on a subset of proteins with similar chain lengths ($180 \leq N < 220$). As shown in Fig. S4F, as ζ decreases, the mean SASA increases, showing the deviation from the perfect globule. Such deviation from the globule will increase the SASA of the molecule, and confer high flexibility to the molecule. For real proteins, it is the solvation/hydration process [7] that plays an important role in the optimization of fluctuation entropy. Experiments and simulations demonstrated that the hydration structure's changes could contribute to protein flexibility and large-amplitude motions of the proteins [8, 9].

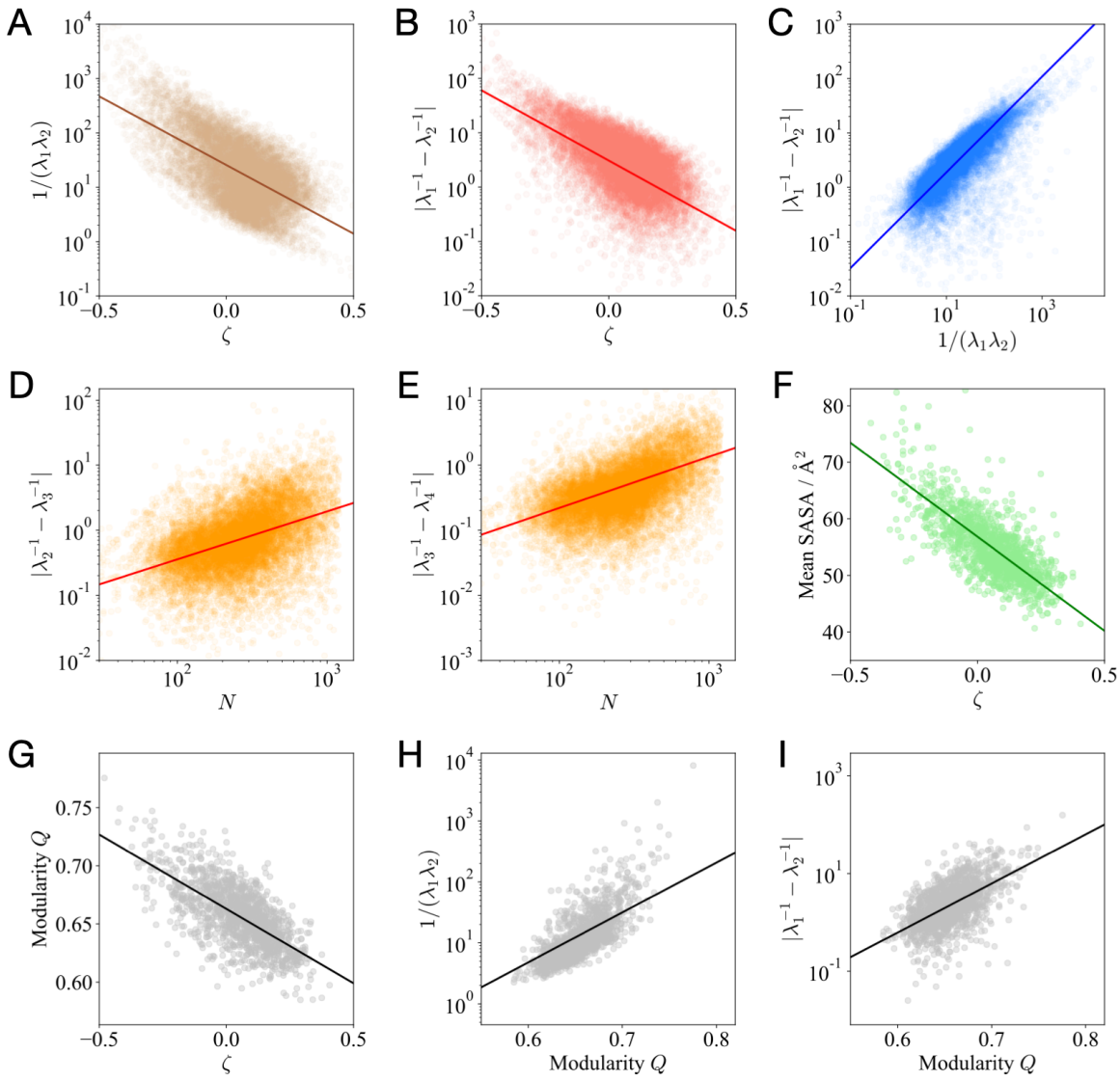

Figure S4: For protein of different sizes, the scattering plots (every data point denotes for a protein) and the trend lines of (A) functional sensitivity $1/(\lambda_1\lambda_2)$ vs the power-law coefficient ζ; (B) mutational robustness $|\lambda_1^{-1}-\lambda_2^{-1}|$ vs ζ; (C) mutational robustness $|\lambda_1^{-1}-\lambda_2^{-1}|$ vs functional sensitivity $1/(\lambda_1\lambda_2)$; (D) eigengap $|\lambda_2^{-1}-\lambda_3^{-1}|$ vs chain length N, and (E) $|\lambda_3^{-1}-\lambda_4^{-1}|$ vs chain length N. For proteins at a similar size (chain length $180 \leq N < 220$), the scattering plot of (F) mean solvent-accessible surface area (SASA) vs ζ, (G) modularity Q vs ζ, (H) functional sensitivity $1/\lambda_1\lambda_2$ vs modularity Q and (I) mutational robustness $\lambda_1^{-1}-\lambda_2^{-1}$ vs modularity Q.

4.2.2 Modularity

Previous research proved that the modularized structures in the residue contact network could contribute to the large-scale motions and slow relaxations of the proteins [5]. Coefficient ζ also correlates with the modularity of the residue contact networks. As shown in Fig. S4G, high modularity Q correlate with small ζ (with negative values). As shown in Fig. S4H and Fig. S4I, for proteins at similar sizes, as modularity Q of the system increases, both product of the eigenvalues $1/(\lambda_1\lambda_2)$ and the eigengap $|\lambda_1^{-1} - \lambda_2^{-1}|$ increase, demonstrating that modularized structures can contribute to both functional sensitivity and mutational robustness.

5 Dataset and Methods: Additional Discussions

5.1 Solvent-accessible Surface Area (SASA)

The solvent-accessible surface area (SASA) defined as the surface area of a protein that is accessible to a water molecule. In this work, we introduced Shrake-Rupley algorithm [10] (embedded in Python Package "MDTraj" [11]) to measure the SASA of the protein molecule.

5.2 Fiedler Vector and Modularity

The Fiedler vector of a graph, namely the eigenvector v_1 corresponding to the smallest non-zero eigenvalue λ_1 of the graph Laplacian matrix, plays an important role in spectral graph partitioning [12, 13]. Based on the sign of the corresponding vector entry, the Fiedler vector v_1 bisects the network into two communities. In the community detection of real-world networks, modularity Q is defined as the fraction of the edges that fall within the given module minus the expected fraction when edges were distributed at random [14, 15]. Such a quantity is designed to quantify if a network can be easily divided into modules. For a network with N nodes and E edges, when the topology is described by the adjacency matrix $\mathcal{A}$, one can introduce the modularity matrix $\mathcal{B}$ with elements $\mathcal{B}_{ij} = \mathcal{A}_{ij} - \frac{k_i k_j}{2E}$ to describe the expected number of edges between node pairs, in which k_i and k_j denote the degrees of node i and j, respectively. Based on matrix $\mathcal{B}$, the modularity can be calculated as: $Q = \frac{1}{4E}\mathrm{Tr}(\vec{x}^T \cdot \mathcal{B} \cdot \vec{x})$, in which $\vec{x}$ is the column vector describing the partition of a network. Vector x has elements $x_i = \pm 1$ indicating the modules to which the node belongs. For any given partition s of a network, one can calculate Q corresponding to such a partition. The appropriate partition of a network would maximize the modularity Q [16]. In this work, we applied the Louvain algorithm [17] to partition the network and maximize the value of modularity Q.

5.3 Dataset

In the file "Protein_Data.txt" (file accessible at: https://bit.ly/37AcczU), the PDB codes for all the proteins in our data set are listed. Besides, the chain length N, radius of gyration R_g, modularity Q, power-law coeffient ζ, spectral dimension d_s, total SASA, mean SASA (SASA per residue), λ_1^{-1}, λ_2^{-1}, functional sensitivity $1/(\lambda_1\lambda_2)$, mutational robustness $|\lambda_1^{-1} - \lambda_2^{-1}|$, $|\lambda_2^{-1} - \lambda_3^{-1}|$, and $|\lambda_3^{-1} - \lambda_4^{-1}|$. All the calculations are based on $r_C = 8$Å.

References

[1] C. Davis and W. M. Kahan. The rotation of eigenvectors by a perturbation. III. *SIAM J. Numer. Anal.* **7**: 1, (1970).

[2] Y. Yu, T. Wang, and R. J. Samworth. A useful variant of the Davis–Kahan theorem for statisticians. *Biometrika* **102**(2): 315 (2014).

[3] S. Reuveni, R. Granek, and J. Klafter. Proteins: Coexistence of Stability and Flexibility. *Phys. Rev. Lett.* 100(20), 208101 (2008).

[4] D. A. Case. Normal mode analysis of protein dynamics. *Curr. Opin. Struct. Biol.* **4**(2): 285-290 (1994).

[5] Q. Y. Tang, K. Kaneko. Long-range correlation in protein dynamics: Confirmation by structural data and normal mode analysis. *PLoS. Comp. Biol.* **16**(2), e1007670 (2020).

[6] J. A. Marsh. Buried and accessible surface area control intrinsic protein flexibility. J. Mol. Biol. **425**(17), 3250-3263 (2013).

[7] H. Frauenfelder, P. W. Fenimore, R. D. Young. Protein dynamics and function: insights from the energy landscape and solvent slaving. *IUBMB life* **59**(8-9): 506-512 (2007).

[8] S. Bone, R. Pethig. Dielectric studies of protein hydration and hydration-induced flexibility. *J. Mol. Biol.* **181**(2), 323-326 (1985).

[9] D. Laage, T. Elsaesser, J. T. Hynes. Water dynamics in the hydration shells of biomolecules. *Chem. Rev.* **117**(16), 10694-10725 (2017).

[10] A. Shrake, J. A. Rupley. Environment and exposure to solvent of protein atoms. Lysozyme and insulin. *J. Mol. Biol.* **79** (2): 351–71 (1973).

[11] R. T. McGibbon, K. A. Beauchamp, M. P. Harrigan, C. Klein, J. M. Swails, C. X. Hernández, *et. al.* MDTraj: a modern open library for the analysis of molecular dynamics trajectories. *Biophys. J.* **109**(8), 1528-1532 (2015).

[12] M. Fiedler, Algebraic connectivity of graphs. *Czech. Math. J.* **23**, 298–305 (1973).

[13] M. E. J. Newman. Finding community structure in networks using the eigenvectors of matrices.*Phys. Rev. E.* **74**(3): 036104 (2006).

[14] M. E. J. Newman, M. Girvan. Finding and evaluating community structure in networks. *Phys. Rev. E.* **69**(2): 026113 (2004).

[15] M. E. J. Newman. Modularity and community structure in networks. *Proc. Natl. Acad. Sci. USA.* **103**(23): 8577-8582 (2006).

[16] M. E. J. Newman. Spectral methods for community detection and graph partitioning. *Phys. Rev. E.* **88**(4): 042822 (2013).

[17] V. D. Blondel, J. L. Guillaume, R. Lambiotte, E. Lefebvre. Fast unfolding of communities in large networks. *J. Stat. Mech.* 2008(10): P10008 (2008).